

## Novel $J_{\text{eff}} = 1/2$ Mott State Induced by Relativistic Spin-Orbit Coupling in $\text{Sr}_2\text{IrO}_4$

B. J. Kim,<sup>1</sup> Hosub Jin,<sup>1</sup> S. J. Moon,<sup>2</sup> J.-Y. Kim,<sup>3</sup> B.-G. Park,<sup>4</sup> C. S. Leem,<sup>5</sup> Jaejun Yu,<sup>1</sup> T. W. Noh,<sup>2</sup> C. Kim,<sup>5</sup> S.-J. Oh,<sup>1</sup>  
J.-H. Park,<sup>3,4,\*</sup> V. Durairaj,<sup>6</sup> G. Cao,<sup>6</sup> and E. Rotenberg<sup>7</sup>

<sup>1</sup>*School of Physics and Astronomy, Seoul National University, Seoul 151-747, Korea*

<sup>2</sup>*ReCOE & School of Physics and Astronomy, Seoul National University, Seoul 151-747, Korea*

<sup>3</sup>*Pohang Accelerator Laboratory, Pohang University of Science and Technology, Pohang 790-784, Korea*

<sup>4</sup>*eSSC & Department of Physics, Pohang University of Science and Technology, Pohang 790-784, Korea*

<sup>5</sup>*Institute of Physics and Applied Physics, Yonsei University, Seoul, Korea*

<sup>6</sup>*Department of Physics and Astronomy, University of Kentucky, Lexington, Kentucky 40506, USA*

<sup>7</sup>*Advanced Light Source, Lawrence Berkeley National Laboratory, Berkeley, California 96720, USA*

(Received 23 January 2008; published 15 August 2008)

We investigated the electronic structure of  $5d$  transition-metal oxide  $\text{Sr}_2\text{IrO}_4$  using angle-resolved photoemission, optical conductivity, x-ray absorption measurements, and first-principles band calculations. The system was found to be well described by novel effective total angular momentum  $J_{\text{eff}}$  states, in which the relativistic spin-orbit coupling is fully taken into account under a large crystal field. Despite delocalized Ir  $5d$  states, the  $J_{\text{eff}}$  states form such narrow bands that even a small correlation energy leads to the  $J_{\text{eff}} = 1/2$  Mott ground state with unique electronic and magnetic behaviors, suggesting a new class of  $J_{\text{eff}}$  quantum spin driven correlated-electron phenomena.

DOI: [10.1103/PhysRevLett.101.076402](https://doi.org/10.1103/PhysRevLett.101.076402)

PACS numbers: 71.30.+h, 71.20.-b, 78.70.Dm, 79.60.-i

Mott physics based on the Hubbard Hamiltonian, which is at the root of various noble physical phenomena such as metal-insulator transitions, magnetic spin orders, high  $T_C$  superconductivity, colossal magneto-resistance, and quantum criticality, has been adopted to explain electrical and magnetic properties of various materials in the last several decades [1–5]. Great success has been achieved in  $3d$  transition-metal oxides (TMOs), in which the localized  $3d$  states yield strongly correlated narrow bands with a large on-site Coulomb repulsion  $U$  and a small band width  $W$ . As predicted, most stoichiometric  $3d$  TMOs are anti-ferromagnetic (AFM) Mott insulators [5]. On the other hand,  $4d$  and  $5d$  TMOs were considered as weakly-correlated wide band systems with largely reduced  $U$  due to delocalized  $4d$  and  $5d$  states [6]. Anomalous insulating behaviors were recently reported in some  $4d$  and  $5d$  TMOs [7–10], and the importance of correlation effects was recognized in  $4d$  TMOs such as  $\text{Ca}_2\text{RuO}_4$  and  $\text{Y}_2\text{Ru}_2\text{O}_7$ , which were interpreted as Mott insulators near the border line of the Mott criteria, i.e.,  $U \sim W$  [7]. However, as  $5d$  states are spatially more extended and  $U$  is expected to be further reduced, insulating behaviors in  $5d$  TMOs such as  $\text{Sr}_2\text{IrO}_4$  and  $\text{Cd}_2\text{Os}_2\text{O}_7$  have been puzzling [8,9].

$\text{Sr}_2\text{IrO}_4$  crystallizes in the  $\text{K}_2\text{NiF}_4$  structure as  $\text{La}_2\text{CuO}_4$  and its  $4d$  counterpart  $\text{Sr}_2\text{RhO}_4$  [8,11]. Considering its odd number of electrons per unit formula ( $5d^5$ ), one expects a metallic state in a naïve band picture. Indeed  $\text{Sr}_2\text{RhO}_4$  ( $4d^5$ ) is a Fermi liquid metal. Its Fermi surface (FS) measured by the angle-resolved photoemission spectroscopy (ARPES) agrees well with the band calculation results [12,13]. Since both systems have identical atomic arrangements with nearly the same lattice constants and bond angles [8,11], one expects almost the same FS topology.

$\text{Sr}_2\text{IrO}_4$ , however, is unexpectedly an insulator with weak ferromagnetism [8]. At this point, it is natural to consider the spin-orbit (SO) coupling as a candidate responsible for the insulating nature since its energy is much larger than that in  $3d$  and  $4d$  systems. Recent band calculations showed that the electronic states near  $E_F$  can be modified considerably by the SO coupling in  $5d$  systems, and suggested a new possibility of the Mott instability [14]. It indicates that the correlation effects can be important even in  $5d$  TMOs when combined with strong SO coupling.

In this Letter, we show formation of new quantum state bands with effective total angular momentum  $J_{\text{eff}}$  in  $5d$  electron systems under a large crystal field, in which the SO coupling is fully taken into account, and also report for the first time manifestation of a novel  $J_{\text{eff}} = 1/2$  Mott ground state realized in  $\text{Sr}_2\text{IrO}_4$  by using ARPES, optical conductivity, and x-ray absorption spectroscopy (XAS) and first-principles band calculations. This new Mott ground state exhibits novel electronic and magnetic behavior, for example, spin-orbit integrated narrow bands and an exotic orbital dominated local magnetic moment, suggesting a new class of the  $J_{\text{eff}}$  quantum spin driven correlated-electron phenomena.

Single crystals of  $\text{Sr}_2\text{IrO}_4$  were grown by flux method [15]. ARPES spectra were obtained at 100 K from cleaved surfaces *in situ* under vacuum of  $1 \times 10^{-11}$  Torr at the beamline 7.0.1 of the Advanced Light Source with  $h\nu = 85$  eV and  $\Delta E = 30$  meV. The chemical potential  $\mu$  was referred to  $E_F$  of electrically connected Au. The band calculations were performed by using first-principles density-functional-theory codes with LDA and LDA +  $U$  methods [16]. The optical reflectivity  $R(\omega)$  was measured at 100 K between 5 meV and 30 eV and the conductivity

$\sigma(\omega)$  was obtained by using Kramers-Kronig (KK) transformation. The validity of KK analysis was checked by independent ellipsometry measurements between 0.6 and 6.4 eV. XAS spectra were obtained at 80 K under vacuum of  $5 \times 10^{-10}$  Torr at the Beamline 2A of the Pohang Light Source with  $\Delta h\nu = 0.1$  eV.

Here we propose a schematic model for emergence of a novel Mott ground state by a large SO coupling energy  $\zeta_{SO}$  as shown in Fig. 1. Under the  $O_h$  symmetry the  $5d$  states are split into  $t_{2g}$  and  $e_g$  orbital states by the crystal field energy  $10Dq$ . In general,  $4d$  and  $5d$  TMOs have sufficiently large  $10Dq$  to yield a  $t_{2g}^5$  low-spin state for  $Sr_2IrO_4$ , and thus the system would become a metal with partially filled wide  $t_{2g}$  band [Fig. 1(a)]. An unrealistically large  $U \gg W$  could lead to a typical spin  $S = 1/2$  Mott insulator [Fig. 1(b)]. However, a reasonable  $U$  cannot lead to an insulating state as seen from the fact that  $Sr_2RhO_4$  is a normal metal. As the SO coupling is taken into account, the  $t_{2g}$  states effectively correspond to the orbital angular momentum  $L = 1$  states with  $\psi_{m_l=\pm 1} = \mp(|zx\rangle \pm i|yz\rangle)/\sqrt{2}$  and  $\psi_{m_l=0} = |xy\rangle$ . In the strong SO coupling limit, the  $t_{2g}$  band splits into *effective* total angular momentum  $J_{\text{eff}} = 1/2$  doublet and  $J_{\text{eff}} = 3/2$  quartet bands [Fig. 1(c)] [17]. Note that the  $J_{\text{eff}} = 1/2$  is energetically higher than the  $J_{\text{eff}} = 3/2$ , seemingly against the Hund's rule, since the  $J_{\text{eff}} = 1/2$  is branched off from the  $J_{5/2}$  ( $5d_{5/2}$ ) manifold due to the large crystal field as depicted in Fig. 1(e). As a result, with the filled  $J_{\text{eff}} = 3/2$  band and

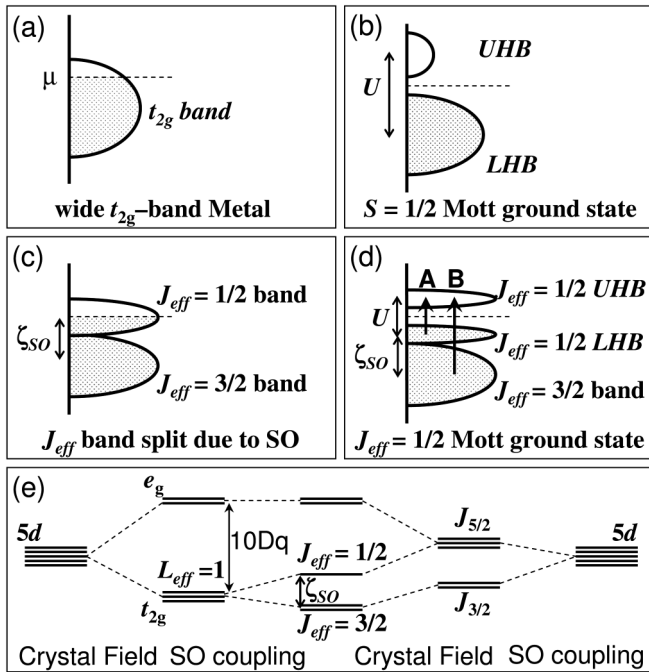


FIG. 1. Schematic energy diagrams for the  $5d^5$  ( $t_{2g}^5$ ) configuration (a) without SO and  $U$ , (b) with an unrealistically large  $U$  but no SO, (c) with SO but no  $U$ , and (d) with SO and  $U$ . Possible optical transitions A and B are indicated by arrows. (e)  $5d$  level splittings by the crystal field and SO coupling.

one remaining electron in the  $J_{\text{eff}} = 1/2$  band, the system is effectively reduced to a half-filled  $J_{\text{eff}} = 1/2$  single band system [Fig. 1(c)]. The  $J_{\text{eff}} = 1/2$  spin-orbit integrated states form a narrow band so that even small  $U$  opens a Mott gap, making it a  $J_{\text{eff}} = 1/2$  Mott insulator [Fig. 1(d)]. The narrow band width is due to reduced hopping elements of the  $J_{\text{eff}} = 1/2$  states with isotropic orbital and mixed spin characters. The formation of the  $J_{\text{eff}}$  bands due to the large  $\zeta_{SO}$  explains why  $Sr_2IrO_4$  ( $\zeta_{SO} \sim 0.4$  eV) is insulating while  $Sr_2RhO_4$  ( $\zeta_{SO} \sim 0.15$  eV) is metallic.

The  $J_{\text{eff}}$  band formation is well justified in the LDA and LDA +  $U$  calculations on  $Sr_2IrO_4$  with and without including the SO coupling presented in Fig. 2. The LDA result [Fig. 2(a)] yields a metal with a wide  $t_{2g}$  band as in Fig. 1(a), and the Fermi surface (FS) is nearly identical to that of  $Sr_2RhO_4$  [12,13]. The FS, composed of one-dimensional  $yz$  and  $zx$  bands, is represented by holelike  $\alpha$  and  $\beta_X$  sheets and an electronlike  $\beta_M$  sheet centered at  $\Gamma$ , X, and M points, respectively [12]. As the SO coupling is included [Fig. 2(b)], the FS becomes rounded but retains the overall topology. Despite small variations in the FS topology, the band structure changes remarkably: Two narrow bands crossing  $E_F$  are split off from the rest due

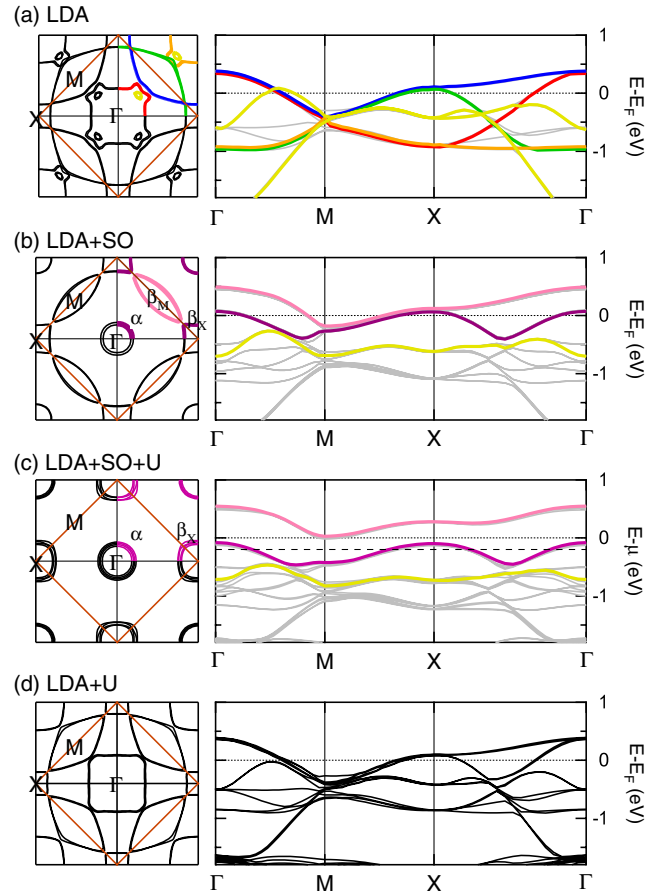


FIG. 2 (color online). Theoretical Fermi surfaces and band dispersions in (a) LDA, (b) LDA + SO, (c) LDA + SO +  $U$  (2 eV), and (d) LDA +  $U$ . In (c), the left panel shows topology of valence band maxima ( $E_B = 0.2$  eV) instead of the FS.

to formation of the half-filled  $J_{\text{eff}} = 1/2$  and filled  $J_{\text{eff}} = 3/2$  bands as shown in Fig. 1(c). The circular shaped FS reflects the isotropic orbital character of the  $J_{\text{eff}} = 1/2$ .

The half-filled narrow band near  $E_F$  suggests that a small  $U$  can lead to a Mott instability. Indeed, a modest  $U$  value opens up a Mott gap and splits the  $J_{\text{eff}} = 1/2$  band into the upper (*UHB*) and lower Hubbard bands (*LHB*), as presented in Fig. 1(d). The *full* LDA + SO +  $U$  results [Fig. 2(c)] manifest the  $J_{\text{eff}} = 1/2$  Mott state. Comparing the LDA + SO and LDA + SO +  $U$  results, one can see that the band gap is opened up by simply shifting up the electronlike  $M$  sheet and down the holelike  $\Gamma$  and  $X$  sheets, yielding a valence band maxima topology as shown in the left panel of Fig. 2(c). It must be emphasized that LDA +  $U$  alone cannot account for the band gap [Fig. 2(d)]. The FS topology changes only slightly from the LDA one, because  $W$  is so large that the small  $U$  cannot play a major role. This result demonstrates that the strong SO coupling is essential to trigger the Mott transition, which reduces to a  $J_{\text{eff}} = 1/2$  Hubbard system.

The electronic structure predicted by the LDA + SO +  $U$  is borne out by ARPES results in Fig. 3. The energy distribution curves (EDCs) near  $\mu$  display band features, none of which crosses over  $\mu$  as expected in an insulator. Figures 3(b)–3(d) show intensity maps at binding energies of  $E_B = 0.2, 0.3,$  and  $0.4$  eV, highlighting the evolution of the electronic structure near  $\mu$ . The first valence band maximum ( $\beta_X$ ) appears at the  $X$  points [Fig. 3(b)]. As  $E_B$  increases [Figs. 3(c) and 3(d)], another band maximum ( $\alpha$ ) appears at the  $\Gamma$  points. The band maxima can also be ascertained in EDCs [Fig. 3(a)]. These results agree well with the LDA + SO +  $U$  results, reproducing the valence band maxima topology (the left panel of Fig. 2(c)). Remarkably, the topmost valence band, which represents the  $J_{\text{eff}} = 1/2$  *LHB*, has small dispersion ( $\sim 0.5$  eV)

although the  $5d$  states are spatially extended and strongly hybridized with the O  $2p$  ones.

The unusual electronic character of the  $J_{\text{eff}} = 1/2$  Mott state is further confirmed in the optical conductivity [18] and the O  $1s$  XAS. The optical conductivity in Fig. 4(a), which shows an  $\sim 0.1$  eV insulating gap consistent with the observed resistivity with an activation energy of 70 meV [19], displays a double-peak feature with a sharp peak A around 0.5 eV and a rather broad peak B around 1 eV. Considering the delocalized  $5d$  states, it is unusual to have such a sharp peak A, which is even narrower than the peaks in  $3d$  TMOs. However, this feature is a natural consequence of the  $J_{\text{eff}}$  Hubbard model depicted in Fig. 1(d). The transitions within the  $J_{\text{eff}} = 1/2$  manifold, from *LHB* to *UHB*, and from the  $J_{\text{eff}} = 3/2$  to the  $J_{\text{eff}} = 1/2$  *UHB* results in the sharp peak A and a rather broad peak B, respectively. A direct evidence of the  $J_{\text{eff}} = 1/2$  state comes from the XAS which enables one to characterize the orbital components by virtue of the strict selection rules [20]. The results in Fig. 4(b) show an orbital ratio  $xy:yz:zx = 1:1:1$  within an estimation error ( $< 10\%$ ) for the unoccupied  $t_{2g}$  state. In the ionic limit, the  $J_{\text{eff}} = 1/2$  states are  $|J_{\text{eff}} = 1/2, m_{J_{\text{eff}}} = \pm 1/2\rangle = (|yz, \pm\sigma\rangle \mp i|zx, \pm\sigma\rangle \mp |xy, \mp\sigma\rangle)/\sqrt{3}$ , where  $\sigma$  denotes the spin state. In the lattice, the intersite hopping, the tetragonal and rotational lattice distortions, and residual interactions with the  $e_g$  states could contribute to off-diagonal mixing between the ionic  $J_{\text{eff}}$  states. However, the mixing seems to be minimal and the observed isotropic orbital ratio, which is also predicted in the LDA + SO +  $U$ , validates the  $J_{\text{eff}} = 1/2$  state.

The  $J_{\text{eff}} = 1/2$  state also contributes unusual magnetic behaviors. The total magnetic moment is dominated by the orbital moment. In the ionic  $J_{\text{eff}} = 1/2$  state, the spin state is a mixture of  $\sigma$  (up spin) and  $-\sigma$  (down spin) and yields  $|\langle S_z \rangle| = 1/6$ . Meanwhile the orbital state yields  $|\langle L_z \rangle| = 2/3$ , resulting in twice larger orbital moment than the spin one, i.e.,  $|\langle L_z \rangle| = 2|\langle S_z \rangle|$ . Note that the  $J_{\text{eff}} = 1/2$  is distinguished from the atomic  $J = 1/2$  ( $|L - S\rangle$ ) with  $L = 1$  and  $S = 1/2$  despite the formal equivalence. The  $J = 1/2$  has a total magnetic moment  $\langle L_z + 2S_z \rangle = \pm 1/3$  with opposite spin and orbital direction ( $L - S$ ), while the  $J_{\text{eff}} = 1/2$  gives  $\langle L_z + 2S_z \rangle = \pm 1$  with parallel one. The  $J_{\text{eff}} = 1/2$  ( $|L_{\text{eff}} - S\rangle$ ) is exactly analogous to the  $J = 1/2$  ( $|L - S\rangle$ ) with mapping  $L_{\text{eff},z} \rightarrow -L_z$ . This is because the  $J_{\text{eff}} = 1/2$  is branched off from the atomic  $J = 5/2$  manifold ( $L + S$ ) by the crystal field, the same reason for the violation of the Hund's rule [Fig. 1(e)]. This aspect differentiates  $5d$  TMOs from  $3d$  TMOs described by spin-only moments and also from rare-earth compounds with atom-like  $J$  states.

The LDA + SO +  $U$  predicts the ground state with weak ferromagnetism resulting from a canted AFM order with an  $11^\circ$  canting angle (net  $22^\circ$ ) in the plane. The predicted local moment is  $0.36\mu_B/\text{Ir}$  with  $0.10\mu_B$  spin and  $0.26\mu_B$  orbital contributions. This value is only about

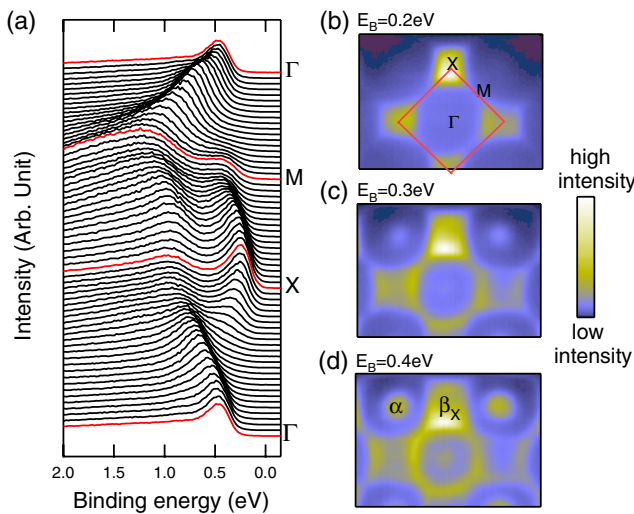


FIG. 3 (color online). (a) EDCs up to  $E_B = 2$  eV along high symmetry lines. (b)–(d) ARPES intensity maps at  $E_B = 0.2, 0.3,$  and  $0.4$  eV. Brillouin zone (small square) is reduced from the original one due to the  $\sqrt{2} \times \sqrt{2}$  distortion.



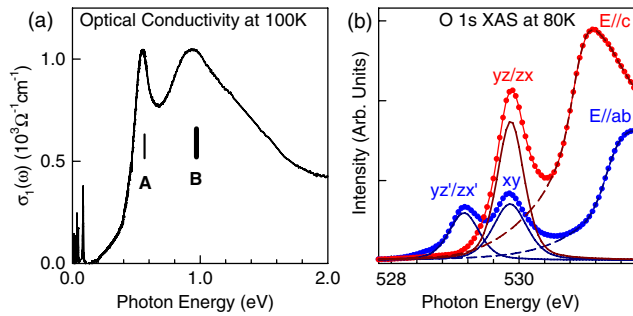


FIG. 4 (color online). (a) Optical conductivity. Peak A and B correspond to transitions denoted in Fig. 1(d). (b) The O 1s polarization dependent XAS spectra (dotted lines) compared with expected spectra (solid lines) under an assumption of  $xy:yz:zx = 1:1:1$  ratio.  $xy$  and  $yz/zx$  denote transitions from in-plane oxygens while  $yz'/zx'$  from apical oxygens, and the energy difference corresponds to their different O 1s core-hole energies [20].

one-third of the ionic value  $1\mu_B$  ( $0.33\mu_B$  spin and  $0.67\mu_B$  orbital ones) for  $J_{\text{eff}} = 1/2$  but still retains the respective ratio close to 1:2. This large reduction, however, seems to be natural since the Ir 5d strongly hybridize with the neighboring O 2p and thus significant parts of the moments are canceled in the AFM order. Indeed,  $\text{Sr}_2\text{IrO}_4$  shows weak ferromagnetism with local moment  $\mu_{\text{eff}} = 0.5\mu_B/\text{Ir}$ , about one-third of  $\mu_{\text{eff}} = 1.73\mu_B$  for  $S = 1/2$ , as determined from the magnetic susceptibility above  $T_C$  [15]. It should be noted that the origin of the canted AFM order is different from that in the spin-based Mott insulators, which is attributed to the spin canting due to the Dzyaloshinskii-Moriya (DM) interaction [21], the first order perturbation term of the SO coupling on the S basis states. But the  $J_{\text{eff}}$  states, in which the SO coupling is fully included, are free from the DM interaction. Their canted AFM order should be explained by the lattice distortion, and the canting angle is indeed nearly identical to that in the Ir-O-Ir bond [8]. Recent Ir L-edge resonant scattering results confirmed the canted AFM order of the  $J_{\text{eff}} = 1/2$  quantum spins in this system [19].

The peculiar electronic and magnetic properties of  $\text{Sr}_2\text{IrO}_4$  can be understood as characteristics of the  $J_{\text{eff}} = 1/2$  Mott insulator. Despite the extended 5d states with a small  $U$ , narrow Hubbard bands with a new quantum number  $J_{\text{eff}}$  different from the atomic  $J$  emerge through the strong SO coupling under the large crystal field. This suggests a new class of materials, namely, spin-orbit integrated narrow band system. The  $J_{\text{eff}} = 1/2$  quantum “spin”, which incorporates the orbital one, is expected to bring in new quantum behaviors. Indeed, recent findings show that many iridates display highly unusual behaviors, for examples, non-Fermi liquid behaviors in  $\text{SrIrO}_3$  [22] and a spin liquid ground state in  $\text{Na}_4\text{Ir}_3\text{O}_8$  [23]. With the relativistic SO coupling, the system is in a new balance of the spin, orbital, and lattice degrees of freedom. It implies that the underlying physics of 5d TMOs is not a simple

adiabatic continuation of the 3d TMO physics to a small  $U$  regime and a new paradigm is required for understanding their own novel phenomena. “What novel phenomena emerge in the vicinity of this new Mott insulator” remains as an open question.

We thank T. Arima and H. Takagi for invaluable discussions. This work was supported by MOST/KOSEF through eSSC at POSTECH, ARP (No. R17-2008-033-01000-0), ReCOE Creative Research Initiative Program, under grant No. R01-2007-000-11188-0, POSTECH research fund, and BK21 program. The work at UK was supported by an NSF Grant No. DMR-0552267. ALS and PLS are supported by the DOE Office of Basic Energy Science and in part by MOST and POSTECH, respectively.

\*Author to whom all correspondence should be addressed.  
jhp@postech.ac.kr

- [1] N. F. Mott, *Metal-Insulator Transitions* (Taylor & Francis, London/Philadelphia, 1990).
- [2] J. Hubbard, Proc. R. Soc. A **276**, 238 (1963).
- [3] P. Fazekas, *Lecture Notes on Electron Correlation and Magnetism* (World Scientific, Singapore, 1999).
- [4] J. G. Bednorz and K. A. Müller, Z. Phys. B **64**, 189 (1986); M. P. A. Fisher and G. Grinstein, Phys. Rev. Lett. **60**, 208 (1988).
- [5] M. Imada, A. Fujimori, and Y. Tokura, Rev. Mod. Phys. **70**, 1039 (1998).
- [6] W. D. Ryden, A. W. Lawson, and C. C. Sartain, Phys. Rev. B **1**, 1494 (1970).
- [7] S. Nakatsuji and Y. Maeno, Phys. Rev. Lett. **84**, 2666 (2000); J. S. Lee *et al.*, Phys. Rev. B **64**, 245107 (2001).
- [8] M. K. Crawford *et al.*, Phys. Rev. B **49**, 9198 (1994).
- [9] D. Mandrus *et al.*, Phys. Rev. B **63**, 195104 (2001).
- [10] R. J. Cava *et al.*, Phys. Rev. B **49**, 11890 (1994); T. Shimura *et al.*, *ibid.* **52**, 9143 (1995).
- [11] T. Vogt and D. J. Buttrey, J. Solid State Chem. **123**, 186 (1996).
- [12] B. J. Kim *et al.*, Phys. Rev. Lett. **97**, 106401 (2006).
- [13] F. Baumberger *et al.* Phys. Rev. Lett. **96**, 246402 (2006).
- [14] D. J. Singh, P. Blaha, K. Schwarz, and J. O. Sofo, Phys. Rev. B **65**, 155109 (2002); K. Rosnagel and N. V. Smith, *ibid.* **73**, 073106 (2006); H. J. Xiang and M.-H. Whangbo, *ibid.* **75**, 052407 (2007).
- [15] G. Cao, J. Bolivar, S. McCall, J. E. Crow, and R. P. Guertin, Phys. Rev. B **57**, R11039 (1998).
- [16] M. Han, T. Ozaki, and J. Yu, Phys. Rev. B **73**, 045110 (2006).
- [17] The XAS confirms that the  $t_{2g}$  level splitting due to lattice distortions is minimal in  $\text{Sr}_2\text{IrO}_4$  [Fig. 4(b)].
- [18] S. J. Moon *et al.*, Phys. Rev. B **74**, 113104 (2006).
- [19] B. J. Kim *et al.* (unpublished).
- [20] T. Mizokawa *et al.*, Phys. Rev. Lett. **87**, 077202 (2001); H.-J. Noh *et al.*, Phys. Rev. B **72**, 052411 (2005).
- [21] I. A. Dzyaloshinskii, J. Phys. Chem. Solids **4**, 241 (1958); T. Moriya, Phys. Rev. **120**, 91 (1960).
- [22] G. Cao *et al.*, Phys. Rev. B **76**, 100402(R) (2007).
- [23] Y. Okamoto, M. Nohara, H. Aruga-Katori, and H. Takagi, Phys. Rev. Lett. **99**, 137207 (2007).